Exact and numerical design of non-polarizing edge filters

Yiqin Ji (季一勤)[1,2*], Deying Chen (陈德应)[1], Huasong Liu (刘华松)[2,3], Zhanshan Wang (王占山)[3], Wei Hong (洪 伟)[2], and Dandan Liu (刘丹丹)[2]

[1] *National Key Laboratory of Tunable Laser Technology, Institute of Opto-electronics, Harbin Institute of Technology, Harbin 150001, China*

[2] *Tianjin Key Laboratory of Optical Thin Films, Tianjin Institute of Jinhang Technical Physics, Tianjin 300192, China*

[3] *Institute of Precision Optical Engineering, Department of Physics, Tongji University, Hanghai 200092, China*

[*] *E-mail: ji_yiqin@yahoo.com*

Received November 16, 2009

Multilayer dielectric thin films have polarization effects at non-normal incidence. In this letter, specifications include s- and p-polarization transmittance ($T_{s,(p)} \geq 95\%$ at 790—808 nm), s- and p-polarization reflectance ($R_{s,(p)} \geq 95\%$ at 814—860 nm), angle of incidence (AOI) = 45°, air as incident medium, and BK7 glass as substrate. Based on the two chosen materials (Ta_2O_5 and SiO_2), non-polarized edge filters are carried out using the design methods of the detuned multiple half-wave filters (exact design) and the needle optimization (numerical design). Exact design has a total of 112 layers and 12 cavities; optical thickness is 126 quartwaves at 860 nm. Numerical design has a total of 107 layers and 8 cavities; optical thickness is 91 quartwaves at 850 nm. Hence, the numerical design has less layers and thickness, thus meeting the same specifications of the exact design.

OCIS codes: 310.5696, 310.4165, 310.5448.
doi: 10.3788/COL201008S1.0025.

At an oblique incidence, admittances and phase thickness of a film were modified[1]. For an absorption-free dielectric, phase thickness has a factor $\cos\theta$, θ is the angle of incidence (AOI) but the admittances have a different factor, $\cos\theta$ for s-polarization and $1/\cos\theta$ for p-polarization, and as such, optical performances of a film obtain polarization effects. Such polarization effects limit the sharpness of edge filters[2,3], Thelen *et al.* successfully devised the principal techniques to improve the sharpness[4,5]. In this letter, exact design (detuned multiple half-wave filters among others) and numerical design (needle optimization among others) of non-polarizing edge filter are discussed and compared.

The techniques devised by Thelen detuned spacer layers of multiple half-wave filters, optimized several layers, mostly spacer layers and the outer two or three layers, and carried out the design to meet the specs. This process is known as exact design. In comparison, techniques like needle optimization or flip-flop optimization set the thicker layer as their starting designs, synthesize with powerful computer and mathematics tools, and finally obtain a design to meet specs. This process is known as numerical design. However, these designs are sometimes said to merely obtain a list of thickness and materials, but no physical significance is achieved.

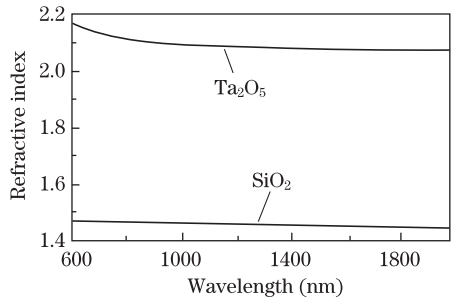

Fig. 1. Refractive indices of Ta_2O_5 and SiO_2 films.

To compare exact and numerical designs, the targets set should include 1) air as the incidence medium and BK7 glass as the substrate; 2) AOI = 45°; 3) T_s and $T_p \geq 90\%$ at 790—807 nm; 4) R_s and $R_p \geq 90\%$ at 817—860 nm.

Before designing, the parameters of films should be exactly known, and as such, the ion beam sputtering (IBS) as the deposition technique, as well as Ta_2O_5 and SiO_2 as the film materials, were chosen. The refractive indices of the films are shown in Fig. 1.

For the configuration,

$$\mathrm{BK7//HLHL}\,\langle\mathrm{Spacer}\rangle\,\mathrm{LHLH//BK7}, \tag{1}$$

where H is the high reflective index layer, L is the low refractive index layer, we have

$$2\Phi_{s,p} + \frac{2\pi}{\lambda_{s,p}} nd\cos\theta = k\pi(k = 0,\ 1,\ 2, ...), \tag{2}$$

where $\Phi_{s,p}$ is the phase of reflection from the spacer, $\lambda_{s,p}$ is the central wavelength of band-pass filter, and s and p are s- and p-polarizations, respectively, n is the refractive index of layer, d is the physical thickness of layer. Furthermore, we can obtain

$$\Delta\Phi = \Phi_s - \Phi_p = \pi nd\cos\theta\left(\frac{1}{\lambda_p} - \frac{1}{\lambda_s}\right). \tag{3}$$

From Fig. 2, $\Delta\Phi \equiv 0$ at normal incidence, and thus, $\lambda_s \equiv \lambda_p$. However, from Fig. 3, $\Delta\Phi \neq 0$ (except for λ_0) at non-normal incidence, and thus, $\lambda_s \neq \lambda_p$(except for λ_0). Thelen *et al.* devised a design to detune multiple half-wave filters to make $\Delta\lambda_c = \lambda_s - \lambda_p \neq 0$. Also, at non-normal incidence, edges of the pass-band become separated as $\Delta\lambda_{s,p}$ due to the effects of polarization. If we can make $\Delta\lambda_c = \pm\Delta\lambda_{s,p}$, then a non-polarizing edge filter is generated.

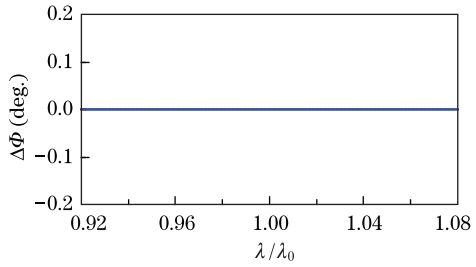

Fig. 2. $\Delta\Phi$ for the configuration BK7//HLHL $\langle$Spacer$\rangle$ at normal incidence.

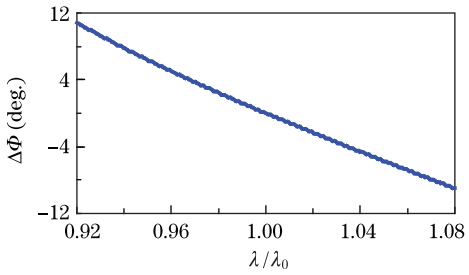

Fig. 3. $\Delta\Phi$ for the configuration BK7//HLHL $\langle$Spacer$\rangle$ at 45° incidence.

Based on the above analysis, for the target, we can have the starting design as

$$\text{BK7//}\left[\text{HLHL2.444HLHLH}\right]^{12}\text{//Air.} \tag{4}$$

To reduce the ripples of pass-band, Eq. (4) can be modified as

$$\text{BK7//}\left[\text{HLH2.458LHLH}\right]^{2}\left[\text{HLHL2.378HLHLH}\right]^{8}\left[\text{HLH2.458LHLH}\right]^{2}\text{//Air.} \tag{5}$$

Then, the design with the software Optilayer is optimized. Figure 4 illustrates the transmittance of Eq. (5), while Fig. 5 shows the transmittance of optimized Eq. (5).

The starting design is only the simple 120H layer and needle optimization by the software Optilayer. Figure 6 is the transmittance of the final design.

Table 1 lists the data comparison of the above exact and numerical designs, which includes the total thickness, merit function (MF), number of layers, and number of cavities. MF and number of layers are almost same, but numerical design has the advantage for both total thickness and number of cavities.

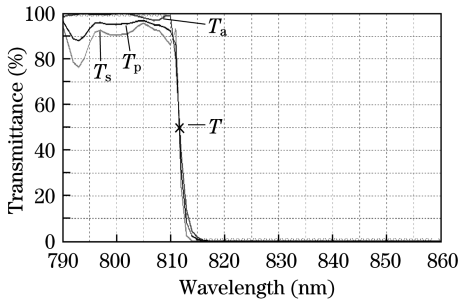

Fig. 4. Transmittance of Eq. (5).

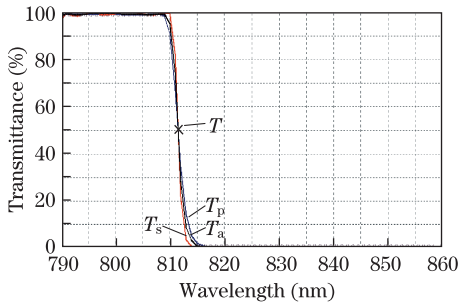

Fig. 5. Transmittance of the optimized Eq. (5).

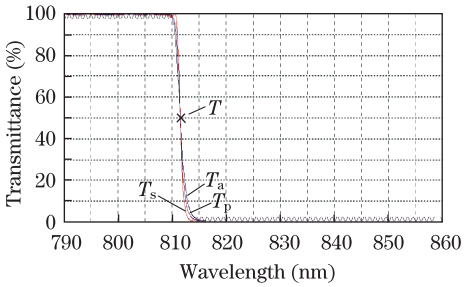

Fig. 6. Transmittance of the final numerical design.

Table 1. Comparison of Exact and Numerical Designs

	Physical Thickness (μm)	MF	Number of Layers	Number of Cavities
Exact design	14.7	0.47	112	12
Numerical design	12.7	0.39	110	8

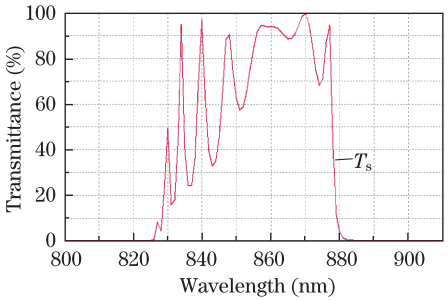

Fig. 7. Transmittance spectrum of the exact design at normal incidence.

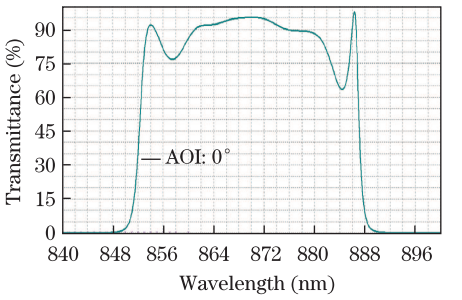

Fig. 8. Transmittance spectrum of the numerical design at normal incidence.

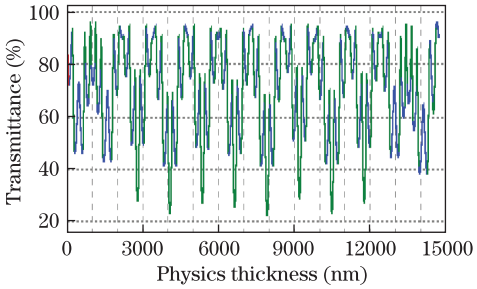

Fig. 9. Simulation of the monochromatic monitoring of the exact design at 860 nm.

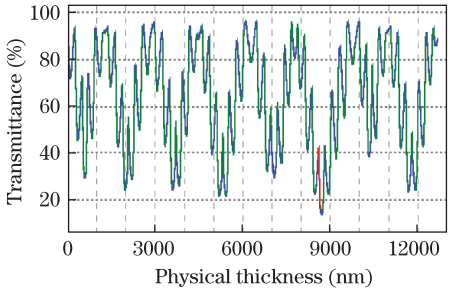

Fig. 10. Simulation of the monochromatic monitoring of the numerical design at 870 nm.

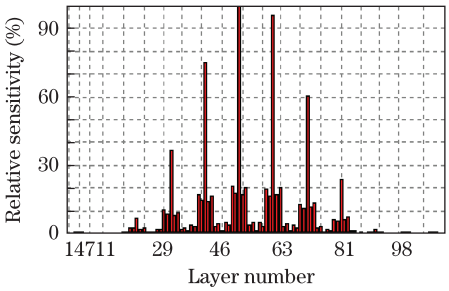

Fig. 11. Layer sensitivity evaluation of the exact design.

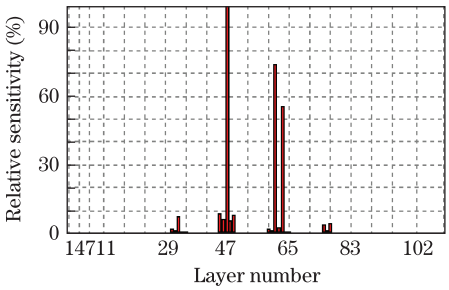

Fig. 12. Layer sensitivity evaluation of the numerical design.

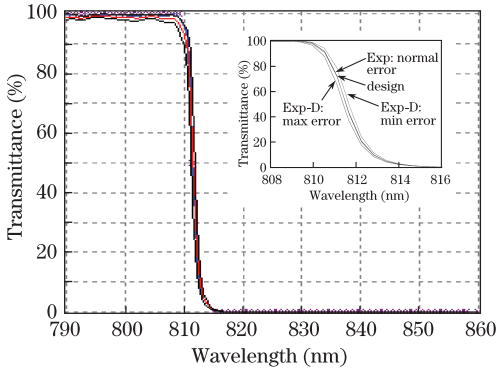

Fig. 13. Error analysis of the exact design.

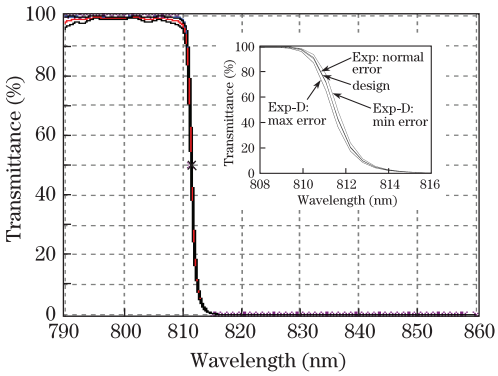

Fig. 14. Error analysis of the numerical design.

Figures 7 and 8 show the transmittance spectra of the designs at normal incidence. Figures 9 and 10 illustrate the simulation of the monochromatic monitoring, showing multiple cavity band pass filters of both designs. Exact design has 12 cavities with the spacer layers being part of the layers, while numerical design has 8 cavities with the spacer layers consisting of two or three sublayers.

Figures 11 and 12 refer to the sensitivity layer evaluation of the designs. Figure 11 is the same as the standard multiple cavity band-pass filter, although the spacer layers are detuned. Meanwhile, Fig. 12 indicates the similarity with the two spacers (3 layers), and thus is most sensitive; it show less than the 3 spacers.

Figures 13 and 14 show the error analysis of the designs wherein relative RMS is 0.2% and probability is 68.3% and re-explain the results of the layer sensitivity evaluation. The corridor width of the edge half-point of exact design is 1 nm. In numerical design, it is only 0.5 nm.

Table 2 is the summary of the layer sensitivity evaluation and the error analysis of the designs.

Table 2. Summary of the Layer Sensitivity Evaluation

	Physical Significance	Layer Sensitivity	Error Analysis
Exact Design	12-cavity band pass filter. All layers are an integral number of quarter wavelength (QW) except for spacers and last two layers.	Spacer layers are sensitive. Central 6 spacers are added. Typical multiple cavity.	When relative root mean square (RMS) = 0.2%, the corridor width of the edge half-point is 1 nm.
Numerical Design	8-cavity band pass filter. All layers are not QW	Similar to multiple cavity, but only two spacers (3 layers) are sensitive.	0.5 nm

In conclusion, aiming at the specific target of the non-polarizing edge filter, a study on the film constructions of the exact and numerical design is carried out prior layer sensitivity evaluation and error analysis. Results of designs, evaluation, and analysis are compared. It is found that the numerical design has an advantage for the specific target.

References

1. H. A. Macleod, *Thin-Film Optical Filters,* Institute of Physics Publishing, Bristol and Philadelphia, 2001.
2. P. Baumeister, Opt. Acta **8,** 105 (1961).
3. K. Rabinovitch and A. Pagis, Opt. Acta **21,** 963 (1974).
4. A. Thelen, Appl. Opt. **15,** 2983 (1976).
5. A. Thelen, J. Opt. Soc. Am. **71,** 309 (1981).